Dual character of excited charge carriers in graphene on Ni(111)

L. Bignardi,[1,*] T. Haarlammert,[2] C. Winter,[2] M. Montagnese,[1,†] P. H. M. van Loosdrecht,[1,†] E. Voloshina,[3] P. Rudolf,[1,‡] and H. Zacharias[2,§]

[1]*Zernike Institute for Advanced Materials, University of Groningen, 9747AG Groningen, The Netherlands*

[2]*Physikalisches Institut, Westfälische Wilhelms-Universität, 48149 Münster, Germany*

[3]*Institut für Chemie, Humboldt-Universität zu Berlin, 12489 Berlin, Germany*

(Received 4 November 2013; revised manuscript received 15 January 2014; published 7 February 2014)

The dynamics of excited charge carriers at the graphene/Ni(111) interface has been investigated by means of time-resolved two-photon photoemission spectroscopy, employing femtosecond-XUV pulses with an energy of 39.2 eV produced by high-order-harmonic generation. Due to the interplay of substrate and adsorbate band structures, the dependence of the lifetimes on the energy ($E - E_F$) of the excited carriers was found to be similar to that of Ni 3*d* electrons measured for clean Ni in the energy range ($E - E_F$) < 1 eV, while it resembled that of graphite from 1 eV above E_F onwards. This result is suggested to be the effect of the peculiar electronic structure of the interface, which still possesses features belonging to the pristine graphene layer, such as a residual saddle point.

DOI: 10.1103/PhysRevB.89.075405 PACS number(s): 73.22.Pr, 42.65.Ky, 79.60.Dp

I. INTRODUCTION

The exploration of the electronic and structural properties of graphene/metal interfaces is from a fundamental point of view particularly interesting because the level of interaction can be tuned by choosing the metallic substrate [1]. This interaction causes, e.g., variations in the work function, different electronic doping of the graphene, and morphological modifications of the graphene, which are important aspects also for future technological applications [1,2].

The graphene (Gr) on Ni(111) system has been of considerable interest recently, both experimentally and theoretically. Angle-resolved photoemission experiments have probed the band structure of occupied electronic states at the interface [3], establishing the hybridization of the π band of graphene with the Ni 3*d* band in the region of the Dirac cone. Due to the perfect matching of the surface lattice parameters of graphene and Ni(111) and since the two Fermi surfaces overlap for one spin orientation only [4], Gr/Ni(111) has been predicted to be a perfect spin filter, suggesting a way to implement spin-valve devices based on such an interface [5,6].

An important topic to explore concerns the characterization of unfilled electronic states and dynamics of excited charge carriers at the Gr/Ni interface, which is relevant to transport phenomena and to device realization. Time-resolved two-photon photoemission (TR-2PPE) using ultrafast laser pulses permits us to directly access, with high precision, the lifetimes and the relaxation dynamics of electronic excitations [7]. Using femtosecond XUV pulses obtained by high-order-harmonic generation (HHG) allows us to probe carrier dynamics in the whole Brillouin zone [8,9], which is particularly important for graphene, as recent experiments proved [10,11]. In this paper we present results of a study on the dynamics of photoexcited charge carriers at the Gr/Ni(111) interface. Valence-band time-resolved pump-probe spectra acquired with visible and XUV pulses reveal that the dynamics is governed by an interplay of the graphene and substrate band structures. The experimental observations are backed by theoretical calculations of the electronic band structure in the interface region.

II. EXPERIMENT

Ultrashort laser pulses were produced by a mode-locked and cavity-dumped Ti:sapphire oscillator, which was amplified by a cryogenically cooled Ti:sapphire amplifier at a repetition rate of 6 kHz. Finally, 35-fs pulses with a central wavelength of 790 nm (1.57 eV) and an energy per pulse of 0.8 mJ were employed. About 5% of this pulse energy served as the pump pulse. The size of the pump beam at the sample was about 0.01 cm^2, resulting in a peak intensity on the sample of about 1.1×10^{11} W/cm^2. The remaining output of the amplifier was focused into an Ar gas target for high-order-harmonic generation. A pair of Mo/Si mirrors were used to select the 25th harmonic at 39.2 eV employed as the probe pulse in the two-photon photoemission experiments since the photoemission cross section for the π states of graphene peaks for that photon energy [12]. The time delay between pump and probe pulses was varied by means of a delay stage, modifying the length of the optical path of the pump. Time-resolved valence-band photoemission spectra were acquired in 10 fs steps by tuning the pump-probe delay in a range between -100 and $+100$ fs.

The time-resolved spectra were recorded by means of a time-of-flight electron spectrometer, consisting of a field-free drift tube terminated with a microchannel plate detector. All spectra shown were acquired at normal emission and at room temperature (300 K). The angular acceptance of the spectrometer was $\pm 2.5^\circ$, which corresponds to an integration over $\Delta k_\parallel = 0.14$ Å^{-1} at $E_{\text{kin}} = 35.6$ eV. Pump and probe beams were focused into an ultrahigh vacuum chamber (base pressure 2×10^{-10} mbar) where a Ni(111) single crystal was attached to a Mo sample holder. The surface of Ni(111) was

*Present address: Physikalisches Institut, Westfälische Wilhelms-Universität, 48149 Münster, Germany; luca.bignardi@gmail.com

†Present address: II. Physikalisches Institut, Universität zu Köln, 50937 Köln, Germany.

‡p.rudolf@rug.nl

§hzach@uni-muenster.de

cleaned with several cycles of Ar^+ ion sputtering ($E_b = 1$ keV) followed by annealing (1080 K).

Graphene was grown in situ by chemical vapor deposition of ethylene on the Ni surface, according to the published procedures [4,13]. The growth occurred at a pressure of 10^{-6} mbar of ethylene, while keeping the crystal at a temperature of 870 K for a few minutes. Low-energy electron diffraction (LEED) on the freshly prepared sample showed a (1×1) pattern due to the almost perfect matching of the graphene and Ni(111) surface lattice parameters. Ultraviolet photoelectron spectra acquired in situ with a commercial He discharge lamp and electron analyzer (Focus CSA300) evidenced the presence of σ and π bands of graphene and were found to be similar to the literature data for single-layer graphene on Ni(111) [3,4].

III. RESULTS AND DISCUSSION

A. XUV pulse characterization

A valence-band spectrum acquired from Gr/Ni(111) with our setup is shown in Fig. 1. The dashed line corresponds to a spectrum recorded with the XUV probe beam. The signal from 3*d* bands of Ni and from π and σ bands of graphene are detected at about 1.5, 6, and 11 eV below the Fermi level. Their positions are found to be consistent with the spectrum acquired with the He discharge lamp and earlier works [4]. The solid line represents a spectrum acquired while pump and probe pulses reach the sample simultaneously, i.e., for a pump-probe delay time of $\Delta t = 0$ fs.

At $\Delta t = 0$ fs, a depletion of the intensity is observed for the Ni 3*d* peak (labeled with α) with respect to the case of the spectrum acquired with the XUV pulse alone. On the other hand, new signals rise alongside the α peak, marked by the upward-pointing arrows and denoted by β and γ. The intensity of these sidebands and the depletion of the intensity of the α peak were found to depend on the pump-probe delay and to be maximized at $\Delta t = 0$. Thus, we infer that the simultaneous arrival of the pump and probe on the sample is responsible for the observed modification in the spectral intensity.

To quantify the observed change in photoemission intensity, the difference in the photoemission signals between the spectra

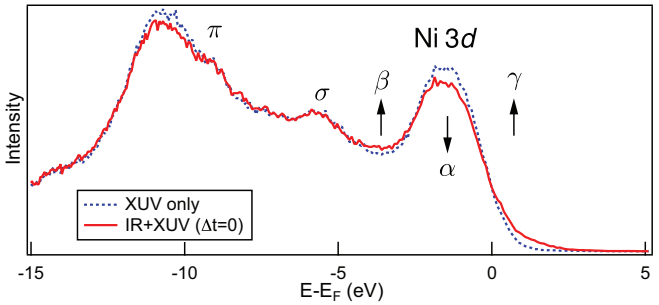

FIG. 1. (Color online) Photoemission spectrum of the valence band of Gr/Ni(111), acquired with a high-order-harmonic-generation setup producing XUV femtosecond pulses with an energy of 39.2 eV. The dashed blue line represents the spectrum acquired with the XUV probe beam only. The red solid line represents the spectrum acquired with the IR pump and XUV probe at a delay time of $\Delta t = 0$ fs.

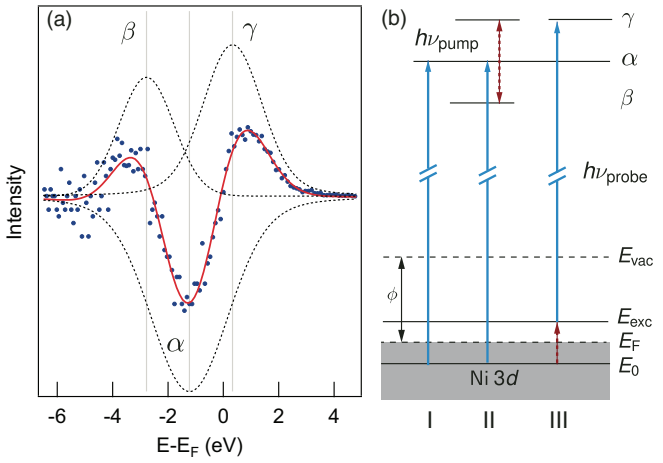

FIG. 2. (Color online) (a) Difference of the photoemission signal between the two spectra shown in Fig. 1 in the vicinity of the Ni 3*d* peak. The blue points are the experimental data, and the red solid line is a fitting plot resulting from the sum of the three dashed-line peaks. (b) Scheme of the photoemission mechanisms involved in the process (see text for explanation). The IR pump and the XUV probe pulses are represented with red dotted and blue solid arrows, respectively.

at $\Delta t = 0$ and acquired with XUV only is calculated, as shown in Fig. 2(a). The difference spectrum (blue dots) is fitted with a convolution of three Gaussian peaks (dashed lines). The fit shows that the decrease in intensity of peak α is compensated by the two rising sidebands β and γ, separated by an energy $h\nu_{\text{pump}} = 1.57$ eV from peak α.

The intensity of the γ sideband appears to be higher than that of the β band, as can be seen in Fig. 2(a). This asymmetry in the intensity of peaks β and γ can be understood considering the photoemission mechanisms resulting in the spectrum at $\Delta t = 0$, sketched in Fig. 2(b). The most prominent process is the direct single-photon photoemission (process I) caused by the XUV pulses, which excite electrons from a state E_0 belonging to the Ni 3*d* band to the α final state.

Moreover, as a consequence of the large intensity of the pump pulse used in this experiment ($\sim 10^{11}$ W/cm^2), we shall consider that the simultaneous arrival of pump and probe pulses on the sample modifies the XUV spectrum and originates an effect known as the laser-assisted photoemission effect (LAPE). Electrons in occupied levels are photoemitted into final states by the XUV photons. However, due to the presence of the intense IR field of the pump pulse, the final states of the photoemitted electrons evolve into free-electron states coupled with the IR field of the pump pulse, known as Volkov states. As a result of this dressing, we observed sidebands that are spaced apart from the main photoemission peak α by exactly the photon energy (1.57 eV) of the pump pulse. Such a feature can be explained as the redistribution of the photoemitted electrons due to the adsorption and stimulated emission of IR photons, originating symmetric sidebands, and it is reported as process II in Fig. 2(b). This mechanism has been observed and successfully explained in photoemission experiments in the gas phase [14] and at solid surfaces [15,16].

The IR pump also produces a distribution of photoexcited electrons that fill unoccupied states at E_{exc} above the Fermi

energy and are then photoemitted by the probe pulses into state γ (process III). We can therefore conclude that a higher intensity of the γ sideband can be explained by the contribution of processes II and III, while the intensity of peak β results only from the LAPE effect. Because of the instantaneous nature of the LAPE signal, the intensity of the sideband β versus the time delay yields the cross-correlation width of the IR and XUV pulses. Accounting for the independently measured duration of the IR pulse (35 ± 10 fs), the duration of the XUV pulse was found to be $\sim 21 \pm 10$ fs.

B. Decay of excited carriers

The complete characterization of the pump and probe pulses allows us to extract information about the transient behavior of the excited carriers from the intensity of the γ peak in the valence band upon a change of the pump-probe time delay. As stated earlier, this peak contains the contributions from a LAPE signal and a distribution of photoexcited carriers in an unfilled state. In the energy range $0.38 < E - E_F < 2.0$ eV the signal was binned into 0.1-eV-wide intervals. The photoemission intensity for each bin was plotted versus the pump-probe delay. As an example the temporal dependence for the bin centered at 0.98 eV is shown in the inset of Fig. 3. The line shape of these curves was fitted with a convolution of the XUV-IR cross correlation (Gaussian) with an exponential decay $\exp[-t/\tau]$, which accounts for the decay of the photoexcited carriers.

Figure 3 shows in a double-logarithmic plot the dependence of the decay rates $\Gamma = 1/\tau$ as a function of the intermediate-state energy $E - E_F$ (red dots). In this plot three regions can be clearly identified. In the energy range $E - E_F < 1$ eV and for $E - E_F > 1.5$ eV, the decay rate Γ is found to increase with increasing energy of the intermediate state. In the range $1 < E - E_F < 1.5$ eV a wide plateau is found where Γ remains flat.

To gain a deeper insight into the energy dependence of the decay rates, we compared the rates observed for Gr/Ni(111) with decay rates measured on nickel [17] and calculated for graphite [18]. In the energy range $E - E_F < 1.0$ eV, the decay rate of Gr/Ni follows $(E - E_F)^n$, with $n = 1.06 \pm 0.06$. This value of n is rather similar to the one extracted for Ni, $n = 1.17 \pm 0.30$, where the decay rate of the excited charge carriers can be modeled by the same expression [17]. The decay rate of excited electrons in graphite shows in this energy range a much stronger dependence on the energy, with an exponent $n = 1.85$.

We therefore conclude that in this energy range the scattering mechanism for the excited carriers in Gr/Ni is similar to metallic Ni. In both cases the observed behavior is different from bulk Fermi-liquid theory, which predicts an exponent of $n = 2$. We also notice that the decay rate measured in Gr/Ni is significantly smaller than that observed for Ni. The lifetime of the excited carriers thus increases when graphene is adsorbed on the metal surface.

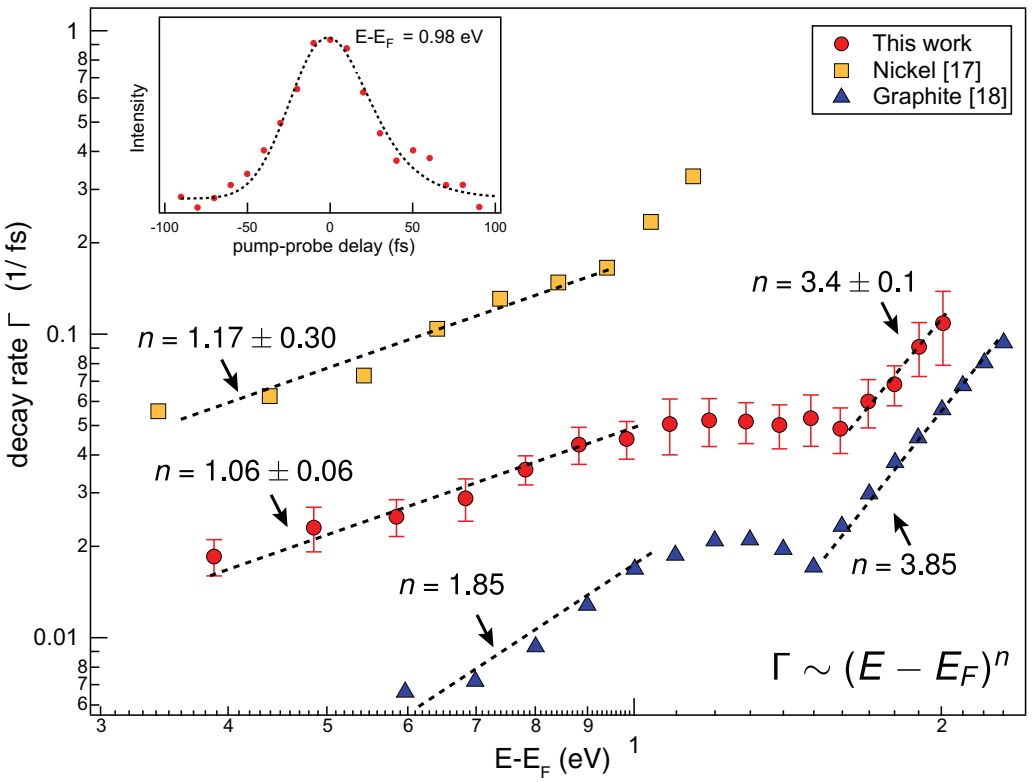

FIG. 3. (Color online) Decay rates Γ of photoexcited electrons plotted vs the energy of the intermediate states (on double-log scale). Red dots refer to Gr/Ni(111), yellow squares refer to nickel [17], and blue triangles refer to graphite [18]. The values of n refer to the energy dependence of the decay rate Γ in the range $E - E_F < 1$ eV and $E - E_F > 1.5$ eV. The inset shows the pump-probe scan curve (dots) while monitoring electrons photoemitted from states at about 0.98 eV above E_F, fitted with a convolution of an exponential decay with the pump-probe cross correlation.

For energies higher than about $E - E_F = 1.5$ eV the decay rate observed for Gr/Ni strongly increases with an exponent of $n = (3.4 \pm 0.1)$. This increase is similar to that theoretically predicted for graphite with $n = 3.85$ [18]. In this energy region the excited carriers clearly behave as graphene electrons. In the energy range $1.0 < E - E_F < 1.5$ eV, a plateau-like region is present in the plot of the decay rates for both Gr/Ni and graphite: the onset of this plateau and its width are unaltered for Gr/Ni with respect to what is predicted [18] and observed [19] for graphite. We therefore conclude that in this energy range the scattering process ruling the decay rates from the excited state is similar in graphite and at the Gr/Ni interface.

The decay rates observed in TR-2PPE experiments directly depend on the shape of the unoccupied electronic bands of the interface, which is important for understanding the scattering mechanism for excited electronic states. Deviations from the bulk Fermi-liquid behavior in transition metals like Ni or Co has been traced to the presence of the partially filled, nondispersive d bands [17,20]. On the other hand, the plateau-like region, observed in the energy dependence of the decay rate [18,19] in highly oriented pyrolytic graphite (HOPG), was directly related to the presence of a van Hove singularity at the M point of the Brillouin zone, located about 1.4 eV above E_F. This resulted in very small decay rates for electronic states located close to the singularity, where many-body effects can become very important [18,21].

Thus, to better understand the mechanism regulating the scattering process of excited charge carriers detailed knowledge of the unoccupied band structure is needed. Density functional theory (DFT) calculations of the band structure and the corresponding C-atom projected density of states for the Gr/Ni(111) interface were carried out. The calculations were performed using the projector augmented-wave method [22], a plane-wave basis set, and the generalized gradient approximation as parameterized by Perdew *et al.* [23], as implemented in the VASP program [24]. The plane-wave kinetic-energy cutoff was set to 500 eV. The long-range van der Waals interactions were accounted for by means of a semiempirical dispersion corrected DFT approach (DFT-D2) proposed by Grimme *et al.* [25]. The supercell used to model the graphene/metal interface was constructed from a slab of 13 layers of nickel atoms with a graphene layer adsorbed at both sides and a vacuum region of approximately 18 Å. In optimizing the structure, the positions (z coordinates) of the carbon atoms as well as those of the top two layers of metal atoms were allowed to relax. In the total energy calculations and during the structural relaxations the k meshes for sampling the supercell Brillouin zone were chosen to be as dense as 24×24 and 12×12, respectively.

The resulting spin-integrated projected density of states (PDOS) for C atoms in Gr/Ni(111) is shown in Fig. 4(b); the calculated projected DOS for graphite is also given [Fig. 4(a)] for comparison. In the region $E - E_F < 1.0$ eV a peak at 0.2 eV is observed, as a result of the hybridization of the graphene unoccupied π^* bands with the unoccupied Ni $3d$ bands. We attribute the Ni-like decay rate observed for Gr/Ni in this energy range to the presence of unfilled Ni bands which are driving the deexcitation process [17,20,26].

Further, a peak in the PDOS of Gr/Ni is predicted at ~1.1 eV above E_F. Within the accuracy of the DFT calculations the energetic position of this peak coincides with the plateau-like region observed for the decay rate of excited charge carriers in Gr/Ni. We attribute this feature to the presence of a residual saddle point in the band structure of the Gr/Ni interface [26], and therefore we conclude that the presence of such a singularity in the DOS affects the decay rate of Gr/Ni, producing a situation similar to what is observed in HOPG [18,19]. As mentioned earlier, the onset of the plateau in the energy dependence of the decay rate in Gr/Ni and in graphite is the same, despite the different PDOS of the two interfaces. This observation suggests therefore that many-body effects are relevant [21,27] in producing electronic states in the energy range $1 < E - E_F < 1.5$ eV, which do not scatter and whose lifetime is greater than expected. At these energies the hot electrons can thus decay only by dissipation of large momenta via the excitation of strongly coupled optical phonons. In graphite fast in-plane vibrations as well as slower c-axis shearing vibrations are excited at Γ (E_{2g}) and K (A_1'), for which large momenta and thus a certain energy of the electrons are required [28–32].

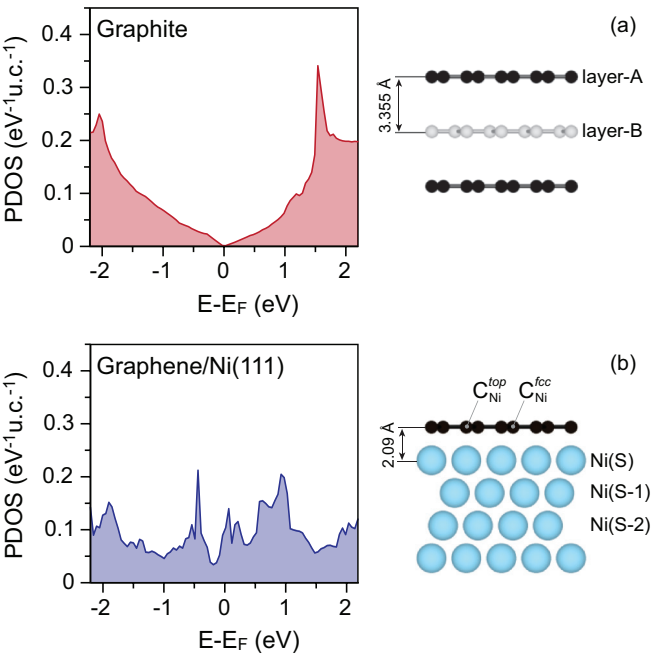

FIG. 4. (Color online) Projected density of states (PDOS) for C atoms calculated (a) for graphite and (b) for the Gr/Ni(111) interface. In each panel a schematic drawing of the model used for the calculations is shown.

The large exponent $n = (3.4 \pm 0.1)$ for $E - E_F > 1.5$ eV reflects then the relaxation within a π^* unoccupied graphene state, with only small momentum dissipation. Further in this energy range the Fermi surface of the interface becomes continuous [4] and therefore provides a larger and increasing phase space for electronic relaxation. Theoretical calculation of the relaxation within this energy range yields an exponent of $n = 3.85$ [18].

In conclusion, we explored the dynamics of excited charge carriers at the Gr/Ni(111) interface by means of a TR-2PPE experiment based on a HHG setup. The decay rates Γ for the excited carriers were extracted by comparison of the

valence-band spectra acquired at different pump-probe time delays. The dependence of the decay rate on the energy of the intermediate state in the energy range $E - E_F < 1$ eV was found to be similar to that measured on clean Ni and thus resembles that of Ni $3d$ electrons. A nearly constant decay rate was observed for intermediate states in the energy range $1 < E - E_F < 1.5$ eV, identical to what is detected for HOPG. We attribute this behavior to the presence of a residual van Hove singularity in the PDOS of Gr/Ni, similar to graphite.

ACKNOWLEDGMENTS

This work was supported by the German Research Foundation (DFG), Priority Program 1459 (Graphene), and by the the "Graphene-based electronics" research program of the Stichting voor Fundamenteel Onderzoek der Materie (FOM), part of the Nederlandse Organisatie voor Wetenschappelijk Onderzoek (NWO). The High Performance Computing Network of Northern Germany (HLRN) is acknowledged for computer time.

[1] M. Batzill, Surf. Sci. Rep. **67**, 83 (2012).
[2] K. S. Novoselov, V. I. Fal'ko, L. Colombo, P. R. Gellert, M. G. Schwab, and K. Kim, Nature (London) **490**, 192 (2012).
[3] A. Varykhalov, J. Sánchez-Barriga, A. M. Shikin, C. Biswas, E. Vescovo, A. Rybkin, D. Marchenko, and O. Rader, Phys. Rev. Lett. **101**, 157601 (2008).
[4] Y. S. Dedkov and M. Fonin, New J. Phys. **12**, 125004 (2010).
[5] V. M. Karpan, G. Giovannetti, P. A. Khomyakov, M. Talanana, A. A. Starikov, M. Zwierzycki, J. van den Brink, G. Brocks, and P. J. Kelly, Phys. Rev. Lett. **99**, 176602 (2007).
[6] V. M. Karpan, P. A. Khomyakov, A. A. Starikov, G. Giovannetti, M. Zwierzycki, M. Talanana, G. Brocks, J. van den Brink, and P. J. Kelly, Phys. Rev. B **78**, 195419 (2008).
[7] H. Petek and S. Ogawa, Prog. Surf. Sci. **56**, 239 (1997).
[8] R. Haight, Surf. Sci. Rep. **21**, 275 (1995).
[9] T. Haarlammert and H. Zacharias, Curr. Opin. Solid State Mater. Sci. **13**, 13 (2009).
[10] J. C. Johannsen, S. Ulstrup, F. Cilento, A. Crepaldi, M. Zacchigna, C. Cacho, I. C. E. Turcu, E. Springate, F. Fromm, C. Raidel, T. Seyller, F. Parmigiani, M. Grioni, and P. Hofmann, Phys. Rev. Lett. **111**, 027403 (2013).
[11] I. Gierz, J. C. Petersen, M. Mitrano, C. Cacho, I. C. E. Turcu, E. Springate, A. Stöhr, A. Köhler, U. Starke, and A. Cavalleri, Nat. Mater. **12**, 1119 (2013).
[12] T. Haarlammert, L. Bignardi, C. Winter, G. Fecher, P. Rudolf, and H. Zacharias, Eur. Phys. J. B **86**, 225 (2013).
[13] C. Oshima and A. Nagashima, J. Phys.: Condens. Matter **9**, 1 (1997).
[14] T. E. Glover, R. W. Schoenlein, A. H. Chin, and C. V. Shank, Phys. Rev. Lett. **76**, 2468 (1996).
[15] L. Miaja-Avila, C. Lei, M. Aeschlimann, J. L. Gland, M. M. Murnane, H. C. Kapteyn, and G. Saathoff, Phys. Rev. Lett. **97**, 113604 (2006).
[16] G. Saathoff, L. Miaja-Avila, M. Aeschlimann, M. M. Murnane, and H. C. Kapteyn, Phys. Rev. A **77**, 022903 (2008).
[17] R. Knorren, K. H. Bennemann, R. Burgermeister, and M. Aeschlimann, Phys. Rev. B **61**, 9427 (2000).
[18] C. D. Spataru, M. A. Cazalilla, A. Rubio, L. X. Benedict, P. M. Echenique, and S. G. Louie, Phys. Rev. Lett. **87**, 246405 (2001).
[19] G. Moos, C. Gahl, R. Fasel, M. Wolf, and T. Hertel, Phys. Rev. Lett. **87**, 267402 (2001).
[20] E. Zarate, P. Apell, and P. M. Echenique, Phys. Rev. B **60**, 2326 (1999).
[21] K. F. Mak, J. Shan, and T. F. Heinz, Phys. Rev. Lett. **106**, 046401 (2011).
[22] P. E. Blöchl, Phys. Rev. B **50**, 17953 (1994).
[23] J. P. Perdew, K. Burke, and M. Ernzerhof, Phys. Rev. Lett. **77**, 3865 (1996).
[24] G. Kresse and J. Hafner, J. Phys.: Condens. Matter **6**, 8245 (1994).
[25] S. Grimme, J. Antony, S. Ehrlich, and H. Krieg, J. Chem. Phys. **132**, 154104 (2010).
[26] E. Voloshina and Y. Dedkov, Phys. Chem. Chem. Phys. **14**, 13502 (2012).
[27] L. Yang, J. Deslippe, C.-H. Park, M. L. Cohen, and S. G. Louie, Phys. Rev. Lett. **103**, 186802 (2009).
[28] R. Saito, A. Jorio, A. G. Souza Filho, G. Dresselhaus, M. S. Dresselhaus, and M. A. Pimenta, Phys. Rev. Lett. **88**, 027401 (2001).
[29] S. Piscanec, M. Lazzeri, F. Mauri, A. C. Ferrari, and J. Robertson, Phys. Rev. Lett. **93**, 185503 (2004).
[30] T. Kampfrath, L. Perfetti, F. Schapper, C. Frischkorn, and M. Wolf, Phys. Rev. Lett. **95**, 187403 (2005).
[31] K. Ishioka, M. Hase, M. Kitajima, L. Wirtz, A. Rubio, and H. Petek, Phys. Rev. B **77**, 121402 (2008).
[32] H. Yan, D. Song, K. F. Mak, I. Chatzakis, J. Maultzsch, and T. F. Heinz, Phys. Rev. B **80**, 121403 (2009).